Phase Behavior and Wall Formation in $Zr(SO_4)_2$/CTABr and $TiOSO_4$/CTABr Mesophases

Mika Lindén,[†] Juliette Blanchard,[‡] Stefan Schacht,[‡] Stephan A. Schunk,[‡] and Ferdi Schüth*[,‡]

Department of Physical Chemistry, Åbo Akademi, Portansgatan 3-5, 20500 Turku, Finland, and Max-Planck-Institut für Kohlenforschung, Kaiser-Wilhelm-Platz 1, 45470 Mülheim, Germany

Received June 23, 1999. Revised Manuscript Received July 16, 1999

The phase behavior of $Zr(SO_4)_2$/CTAB composite mesophases was investigated as a function of surfactant chain length, temperature, and salt concentration by XRD. It was shown that the initial step is a rapid formation of either a pure lamellar, hexagonal, or a mixed hexagonal/lamellar phase with a low degree of condensation (room temperature), depending on the chain length of the surfactant as well as on the ionic strength of the solution. The observed features may be qualitatively explained by expected variations in the packing parameter. $TiOSO_4$/CTAB composite mesophases were shown to form in a similar manner as $Zr(SO_4)_2$/CTAB. A model accounting for changes in the inorganic framework with increasing degree of intraaggregate condensation was developed. Furthermore, using a tubular reactor setup connected to an in situ XRD cell it was shown that the mesophase formation occurred immediately (<300 ms) after mixing of the reagents, which is the fastest ever recorded composite mesophase formation.

Introduction

Since the discovery in 1992 that well-ordered mesoporous silica with pore sizes in the range 20−100 Å could be synthesized using organized organic assemblies as templates,[1,2] this class of materials has attracted a wide interest. A lot of effort has been invested to understand the mechanism of formation of these materials. The resemblance between the observed silica−surfactant composite mesophases and those observed in surfactant−water solutions suggests that the driving forces responsible for the mesophase formation are similar in both cases. The free energy of surfactant self-assembly in dilute solutions consists of three terms:[3] (i) a favorable hydrophobic interaction due to the hydrocarbon chains sequestering themselves within the interior of the aggregates, (ii) a surface term reflecting the opposing tendencies of surfactant headgroups to agglomerate together to minimize hydrocarbon−water contact while simultaneously charge repulsion, hydration, and steric effects force them apart, and (iii) a packing term which accounts for the exclusion of water and surfactant headgroups from the hydrophobic interior of the aggregates.

For dilute surfactant solutions where interaggregate interactions are of minor importance a model has been developed[4] to correlate the molecular geometry of the individual surfactant monomer to the observed aggregate structures. The surfactant number, N_s, is defined as

$$N_s = v/la_o$$

where v is the volume of the hydrophobic tail, l is the effective length of the surfactant, and a_o is the effective area of the hydrophilic headgroup. For N_s values of 0.33, 0.5, and 1, spherical, rodlike, and lamellar geometries are expected to form, respectively. For ionic surfactants the value of a_o is strongly dependent on the degree of dissociation of the headgroups and the ionic strength of the solution. Furthermore, for surfactants with the same headgroup, an increase in the hydrocarbon chain length will favor structures with lower curvature.

Monnier et al.[5] introduced multidentate binding of silicate oligomers, preferred polymerization of silicate at the surfactant−silicate interface and charge density matching as key factors in the formation of a surfactant−silicate mesophase. It is suggested that the final structure of the mesostructure is determined by the interplay of forces acting in the inorganic−inorganic, inorganic−organic, and organic−organic interfacial regions. This model qualitatively explains the occasionally observed transitions from lamellar to hexagonal symmetry for composite mesophases. While early stages of mesostructure formation are determined mainly by the

* To whom correspondence should be addressed.
[†] Åbo Akademi.
[‡] Max-Planck-Institut für Kohlenforschung.

(1) Kresge, C. T.; Leonowicz, M. E.; Roth, W. J.; Vartuli, J. C. *Nature* **1992**, *359*, 710.
(2) Beck, J. S.; Vartuli, J. C.; Roth, W. J.; Leonowicz, M. E.; Kresge, C. T.; Schmitt, K. D.; Chu, C. T.-W.; Olson, D. H.; Sheppard, E. W.; McCullen, S. B.; Higgins, J. B.; Schlenker, J. L. *J. Am. Chem. Soc.* **1992**, *114*, 10834.
(3) Evans D. F.; Wennerström, H. *The Colloidal Domain*; VCH Publishers: New York, 1994; p 12.
(4) Israelachvili, J. N.; Mitchell, D. J.; Ninham, B. W. *J. Chem. Soc., Faraday Trans. 2* **1976**, *72*, 1525.
(5) Monnier, A.; Schüth, F.; Huo, Q.; Kumar, D.; Margolese, D.; Maxwell, R. S.; Stucky, G. D.; Krishnamurty, M.; Petroff, P.; Firouzi, A.; Janicke M.; Chmelka, B. F. *Science* **1993**, *261*, 1299.

10.1021/cm991082x CCC: $18.00
Published on Web 09/11/1999

surfactant properties, further structural phase transformations to lower energy configurations may be induced as changes in the charge density of the silicate occurs upon condensation. The charge density of the silicate framework is expected to decrease upon condensation under alkaline conditions, forcing the surfactants to adopt geometries with increased averaged headgroup areas, i.e., to geometries with a higher curvature. This implies that the inorganic part of the composite plays an important role in determining the final structure of the mesophase. In fact, reversible lamellar−hexagonal phase transitions may also be induced by changes in temperature at pHs high enough for condensation reactions not to occur.[6] This allows a decoupling of aggregation and condensation and gives clear evidence for the importance of the dynamic forces acting between ion-pair inorganic and organic species.

Numerous attempts to extend the synthesis to ordered non-siliceous mesoporous structures have been reported. However, in the initial phase, in most cases removal of the template had not been possible without breakdown of the mesostructure, with only few exceptions.[7−9] This observation has been attributed to the noncondensed nature of the inorganic framework for the tungsten compound,[10] suggesting that the mesophase formation in some of these systems is rather the result of an organic−inorganic salt-pairing. The occurrence of more than one stable oxidation state is thought to lead to subsequent framework collapse during thermal template removal due to oxidation/reduction processes. Furthermore, the ability of the inorganic precursor to form polyoxoions in solution able to undergo further condensation is thought to be a prerequisite for the formation of stable mesostructures. Stable, mesoporous sulfated ZrO_2 has been synthesized by Ciesla et al. using $Zr(SO_4)_2$ as the inorganic precursor.[7,11] Subsequently other groups have also been successful in obtaining mesoporous ZrO_2.[9,12−14] Zirconium readily forms polyoxo ions in solution and exhibits only one stable oxidation state, which means that reduction by the surfactant during calcination or oxidation by air oxygen leading to structural breakdown is unlikely to occur. Zirconium sulfate forms polymeric $[Zr(OH)_2SO_4(OH_2)]$ units in water which are capable of cross-linking through sulfate bridges.[15] It is thought that electrostatic surfactant−sulfate interactions are responsible for the formation of the Zr/CTAB mesophase. While effort has been made in understanding formation of siliceous mesostructures, little work has been carried out to elucidate the processes by which non-siliceous materials assemble. Mesostructures of Zr and Ti are ideal systems for this kind of study, since condensation reactions are relatively slow at room temperature, which makes it easier to distinguish between structural changes originating from template−inorganic interactions and those induced by inorganic−inorganic interactions. This has been achieved for silica by using cubic octamers as the major silicate species in solution.[16] In this study, we report data, which give insight in processes occurring during the formation of non-siliceous mesophases, obtained by in situ and ex situ XRD carried out at different stages of $Zr(SO_4)_2$/CTABr mesophase formation. Here, surfactant chain length, salt concentration, and temperature were used as variables. Computer simulation of the diffractograms was used in the development of a model of wall formation. $TiOSO_4$/CTAB composite mesophases were also studied in order to verify the proposed formation mechanism.

Experimental Section

Tetradecyl-, hexadecyl-, or octadecyltrimethylammonium bromide (Aldrich) were used as templates. Octadecyltrimethylammonium bromide was recrystallized at least three times in ethanol−acetone before use. $Zr(SO_4)_2$ (Alfa) >99% and $TiOSO_4{\cdot}xH_2SO_4{\cdot}xH_2O$ (Aldrich) TiO_2 content of 33 wt % (estimated by heat loss at 1000 °C) were used as supplied. A total of 6.87 mmol of the template was dissolved in 50 g of H_2O to which 0.0128 mol $Zr(SO_4)_2$ or $TiOSO_4{\cdot}xH_2SO_4{\cdot}xH_2O$ dissolved in 50 g of H_2O was added. Immediate precipitation of a white solid occurred upon mixing. The precipitate was isolated immediately after mixing or after different times of heating at 90 °C (reflux) under stirring (250 rpm).

A STOE STADI P transmission X-ray diffractometer with a position sensitive detector with an aperture of 5° 2θ (PSD) was used for all XRD experiments. Wet samples were analyzed in all cases to avoid phase transitions induced by drying of the sample. The ex situ XRD measurements were carried out using either traditional transmission XRD sample holders or a measurements cell especially designed for the measurement of liquid samples built in house. The tubular reactor setup used for in situ XRD measurements has been described elsewhere.[17] The liquid cell was used for all in situ experiments. No fouling on the cell windows during the course of the experiment could be detected.

The chemical formulas of the zirconia mesophases were evaluated from the Zr/S ratio and the ZrO_2 content supposing the following raw formula $Zr(SO_4)_x(CTAB)_yO_{2-x/2}$. The Zr/S ratios were determined with a X-ray fluorescence analysis using a PW 1400 Philips system. The oxide contents of the samples were estimated from the weight loss at 1000 °C.

Results

An immediate precipitation of a white powder is observed upon mixing of the aqueous solution of $Zr(SO_4)_2$ and that of the template. To determine the structural evolution of Zr/C_nTABr (n = 14, 16, 18) mesophases during synthesis, XRD patterns were measured on wet samples taken immediately after mixing of the reagents at 35 °C and after different times of heating in the mother liquid at 90 °C. The measured diffractograms for Zr/C_{14}TABr are shown in Figure 1. It is evident that a composite mesophase has formed

(6) Stucky, G. D.; Monnier, A.; Schüth, F.; Huo, Q.; Margolese, D.; Kumar, D.; Krishnamurty, M.; Petroff, P.; Firouzi, A.; Janicke, M.; Chmelka, B. F. *Mol. Cryst. Liquid Cryst.* **1994**, *240*, 187.
(7) Ciesla, U.; Schacht, S.; Stucky, G. D.; Unger, K. K.; Schüth, F. *Angew. Chem., Int. Ed. Engl.* **1996**, *35*, 541.
(8) Antonelli, D. M.; Ying, J. Y. *Curr. Opin. Colloid Interface Sci.* **1996**, *1*, 523.
(9) Liu, B.; Reddy, J. S.; Adnot, A.; Sayari, A. *Mater. Res. Soc. Symp. Proc.* **1996**, *431*, 101.
(10) Stein, A.; Fendorf, M.; Jarvie, T. P.; Mueller, K. T.; Benesi, A. J.; Mallouk, T. E. *Chem. Mater.* **1995**, *7*, 304.
(11) Ciesla, U.; Fröba. M.; Stucky, G. D.; Schüth, F. *Chem. Mater.* **1999**, *11*, 227.
(12) Wong, M. S.; Antonelli, D. M.; Ying, J. Y. *Nanostrut. Mater.* **1997**, *9*, 165.
(13) Pacheco, G.; Zhao, M.; Garcia, A.; Sklyarov, A.; Frypiat, J. J. *Chem. Commun.* **1997**, 491.
(14) Wong, M. S.; Ying, J. Y. *Chem. Mater.* **1998**, *18*, 2067.
(15) Livage, J.; Henry, M.; Sanchez, C. *Prog. Solid State Chem.* **1988**, *18*, 259.
(16) Firouzi, A.; Atef, F.; Oertli, A. G.; Stucky, G. D.; Chmelka, B. F. *J. Am. Chem. Soc.* **1997**, *119*, 3596.
(17) Lindén, M.; Schunk, S. A.; Schüth, F. *Angew. Chem., Int. Ed. Engl.* **1998**, 110, 871.

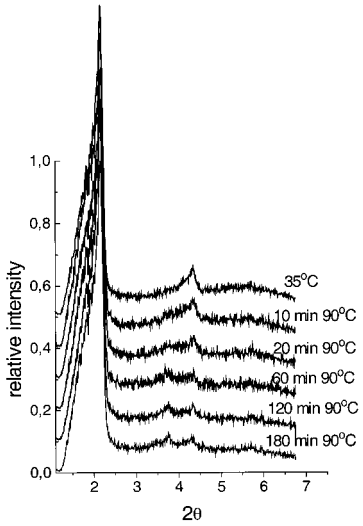

Figure 1. Series of diffractograms for $C_{14}TABr/Zr(SO_4)_2$ recorded at different reaction times. The corresponding times and temperatures are indicated.

upon mixing of the reactants. Only two low-angle reflections were clearly resolved, the second being a higher order reflection of the first one. The *d* spacing was 40.7 Å and did not change during the reaction. However, a third reflection appeared if the reaction solution was kept at 90 °C, the intensity of which increased with time. After about 2 h of heating, the intensity of this reflection exceeded that of the initially observed high order reflection. The reflections could now be assigned assuming a hexagonal symmetry, with the intensity of the (110) reflection being higher than for the (200) reflection, as normally observed for MCM-41 type materials. Reactions with equal $Zr/CTABr/H_2O$ ratios were also carried out in the presence of HCl ($c \leq 0.4$ M). Low HCl concentrations favor the formation of highly viscous, glue-like suspensions which do not settle easily, whereas high HCl content leads to gritty precipitates. Addition of HCl caused a slight increase in the *d* spacing to 41.6 Å, which lies within the experimental deviations for different samples.

The corresponding diffractograms observed for $Zr/C_{16}TABr$ are shown in Figure 2. In contrast to what was observed for $Zr/C_{14}TABr$, all three reflections were now clearly resolved even for the unheated sample and could be indexed assuming a hexagonal symmetry. The observed *d* spacing was 44.6 Å in agreement with the longer hydrocarbon chain length of $C_{16}TABr$ compared to $C_{14}TABr$. Again the *d* spacing stayed virtually constant during the reaction. However, the intensity of the (110) reflection was initially lower than that of the (200) reflection, and again the intensity ratio was inverted with prolonged heating time. The kinetics of this process was similar to what was observed for $Zr/C_{14}TABr$, after 2 h of heating the intensities of the high order reflections equaled those expected for a MCM-41-type material. As for $Zr/C_{14}TABr$, addition of 0.4 M HCl did not affect the kinetics of the reaction but a slight increase in *d* spacing to 45.7 Å was observed.

A clearly different phase behavior was observed for $Zr/C_{18}TAB$ as shown in Figure 3. Here a mixed hexagonal/lamellar phase forms upon mixing of the reagents as evidenced by the presence of two separate (100) and (001) reflections. The corresponding *d* spacings were

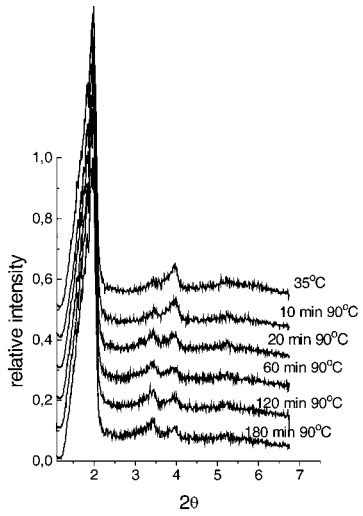

Figure 2. Series of diffractograms for $C_{16}TABr/Zr(SO_4)_2$ recorded at different reaction times. The corresponding times and temperatures are indicated.

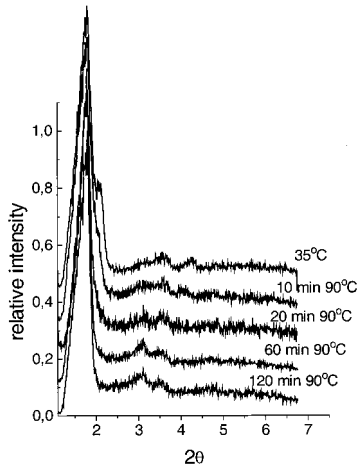

Figure 3. Series of diffractograms for $C_{18}TABr/Zr(SO_4)_2$ recorded at different reaction times. The corresponding times and temperatures are indicated.

42.2 and 48.7 Å for the lamellar and the hexagonal phase, respectively. The mixed phase gradually converts to a pure hexagonal structure upon heating as evidenced by the disappearance of the (001) and (002) reflections. Again, the intensity of the hexagonal (110) reflection increases with time to finally exceed the intensity of the (200) reflection.

Samples were taken from the reaction mixture immediately after mixing ("as made" sample) and after 8 h aging at 90 °C ("thermally treated" sample). They were filtered, washed twice with deionized water, and dried at room temperature for 24 h. The thermal treatment led to a decrease of the sulfate/zirconium and the surfactant/zirconium ratio, as seen from the chemical composition of the "as made" sample, $Zr(Surf)_{0.70}(SO_4)_{0.61}O_{1.65}$, and of the "thermally treated" sample, $Zr(Surf)_{0.55}(SO_4)_{0.47}O_{1.75}$. If 0.4 M HCl was added to the reaction mixture, only a lamellar phase with a *d* spacing of 44.4 Å was observed after mixing of the reagents, as shown in Figure 4. Upon heating, a gradual transition to a hexagonal structure is observed although some traces of the lamellar phase are still seen in the diffractogram of a sample held at 90 °C for 45 h. To exclude the possibility that the observed differences

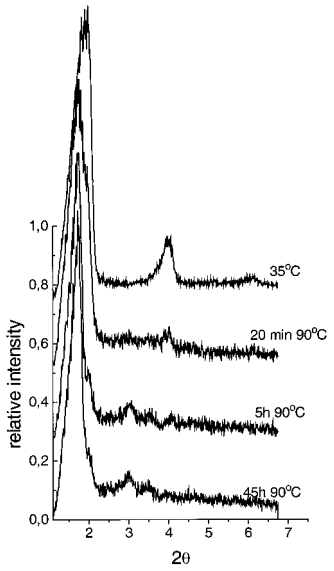

Figure 4. Series of diffractograms for C_{18}TABr/HCl/$Zr(SO_4)_2$ recorded at different reactions times. The corresponding times and temperatures are indicated.

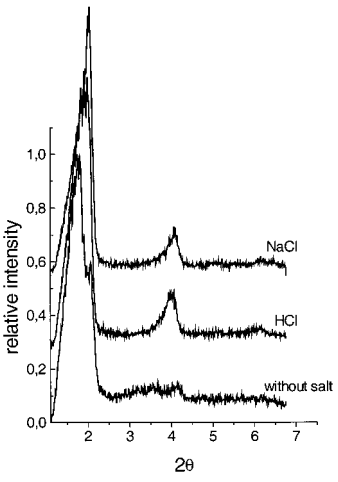

Figure 5. Series of diffractograms for C_{18}TABr/$Zr(SO_4)_2$ recorded with different additives. The corresponding additives are indicated.

arise from the formation of different Zr species in solution in the presence of HCl, a similar reaction was carried out substituting HCl for NaCl ($c = 0.4$ M). Again a purely lamellar structure with a *d* spacing of 43.2 Å was observed as shown in Figure 5, suggesting that it is the increase in the ionic strength of the solution which is responsible for converting the system from a mixed hexagonal/lamellar structure into a purely lamellar one.

A similar reaction was carried out substituting Zr-$(SO_4)_2$ for $TiOSO_4$ and using C_{16}TABr as the template. The measured diffractograms are shown in Figure 6. A Ti/C_{16}TABr mesophase similar to that observed for Zr/C_{16}TABr formed already at room temperature. However, the *d* spacing was 47.7 Å for Ti/C_{16}TAB compared to 44.6 Å for Zr/C_{16}TABr. The evolution of the diffractograms with time is in qualitative agreement with those observed for Zr/C_{16}TABr. However, the higher intensity of the (110) reflection compared to the (200) reflection was now observed already after a heating time of 20 min, compared to ~120 min for Zr/C_{16}TABr.

Neither the zirconia- nor the titania-based materials are stable upon calcination as such. However, both

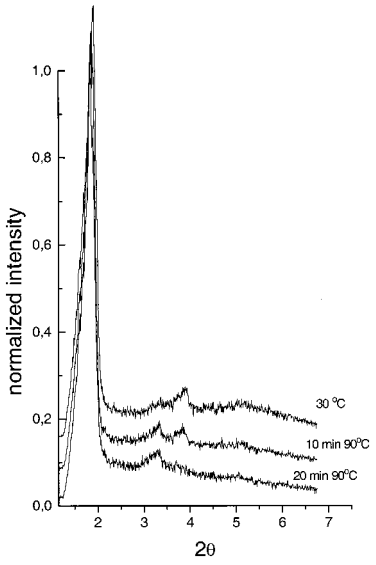

Figure 6. Series of diffractograms for C_{16}TABr/$TiOSO_4$ recorded at different reaction times. The corresponding times and temperatures are indicated.

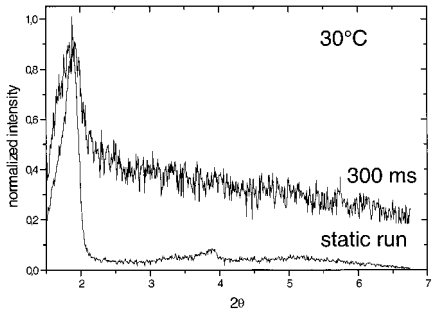

Figure 7. Comparison between a diffractogram obtained after short synthesis times in a single batch experiment for the C_{16}-TABr/$TiOSO_4$ system (static run) and a diffractogram obtained in an in situ experiment with a tubular reaction system at a residence time of 300 ms.

materials can be calcined, if treated with phosphate, as described in refs 7 and 11. Such a treatment results in oxophosphates of the metals which are stable up to 600 °C in the case of zirconium and ~500 °C in the case of titanium. Depending on chain length of the surfactants, the samples are either microporous or have pores in the lower mesopore range.

To investigate the kinetics of mesophase formation in these systems a tubular reactor setup was developed especially for studying fast reactions,[17] allowing data accumulation times long enough to increase the signal-to-noise ratio. Two peristaltic pumps were connected to a XRD cell designed for in situ measurements on liquid samples. An aqueous solution of $TiOSO_4$ and C_{16}TABr, respectively, were mixed (volume ratio 1:1) just before entering the cell, which allowed continuous data collection of the forming dispersion at reaction times shorter than 300 ms. The diffractogram thus obtained is shown in Figure 7. Although the signal-to-noise ratio is not good and no high order reflections can be resolved, it is evident that mesophase formation occurs immediately after mixing. Zr solutions gave essentially similar results, but with an even worse signal-to-noise ratio due to the strong scattering and absorption of the zirconium-containing solutions. No low-angle reflection was observed for the pure surfactant solution. The position of

the low-angle reflection coincides with that observed in the ex situ measurements on the wet samples, suggesting that the structure is similar in both cases. This is the fastest ever recorded mesophase formation for inorganic−organic composites and demonstrates the applicability of the tubular reactor setup in studying reactions with fast kinetics. The result suggests, that the delay of about 90 s after mixing observed in the formation of silica based mesophases[17] is not due to a slow assembly, but rather caused by the slower hydrolysis of the tetraethoxysilane employed in that study as opposed to the transition metal precursors used here.

Discussion

It would be tempting to interpret the initial low intensity of the (110) compared to the (200) reflection observed for Zr/C_{14}TABr and Zr/C_{16}TABr to correspond to a lamellar structure. However, the position of the (100) reflection remains constant which would not be the case if a true lamellar-to-hexagonal transition would occur, since while $a = d$ for a lamellar symmetry $a = 2d/3^{1/2}$ for a hexagonal symmetry. Such a true lamellar-to-hexagonal transition has also been frequently observed in this study, for instance in Figure 4, but is quite different to the change in intensities described above. In these cases the hexagonal mesophase forms already at room temperature and the changes in the relative intensities of the observed reflections originate from restructuring of the inorganic framework during condensation. A model was developed to explain this peculiar feature of the diffractograms, i.e., a gradual increase in the intensity of the (110) reflection upon heating. This model supplements the models proposed by Chen et al.[18] and Monnier et al.[5] in that it adds to a more detailed understanding of how the pore walls are formed. Irrespective of whether the assembly forms according to the Chen et al. model, where inorganic species adsorb to rodlike micelles which then assemble, or whether the mesophase is formed according to Monnier et al. in a cooperative process, it is clear that the assembly can be very rapid, and in the initial phase is most probably governed by the surfactant packing parameter. Thus, either hexagonal assemblies are formed directly, as seen in Figure 1, or, at higher ionic strength, lamellar structures form, as seen in Figure 4. Due to the slower condensation of the transition metal species compared to silicates, the composite aggregates behave similar to normal surfactant aggregates in mesophases built up of individual monomers. Subsequent changes in the mesostructure due to condensation of the inorganic framework are best described by the charge density matching model introduced by Monnier et al.[5] and extended in a subsequent paper also from the Stucky group.[19]

The development of the wall structure for a system where the initially formed mesophase is hexagonal is shown in Figure 8. Due to the highly flexible nature of a composite mesostructure at a low degree of condensation, the aggregates will behave similar to normal surfactant aggregates and the hexagonal mesophase consists of close-packed round rodlike composite aggregates. However, when the degree of condensation increases, the geometry will gradually change due to inter- and intraaggregate condensation to maximize inorganic−inorganic contact. As seen in Figure 8 this structural change will increase the amount of inorganics (good scatterers) along the (110) axis, while no strong change in scatterer density along the (100) (or (200)) axis occurs. Therefore we believe that this model accounts for the observed increase in the intensity of the (110) reflection upon heating. A similar development might also take place in the silica case, but would be more difficult to detect due to the smaller scattering power of the silica compared to the transition metal species. Although the formation of hexagonally shaped pores would result in an energetically favorable constant wall thickness, we do not have any evidence at the time proving that this is the case. However, the intensity of the (110) reflection is not dependent on the geometry of the pore but on the total density of scatterers along the (110) axis.

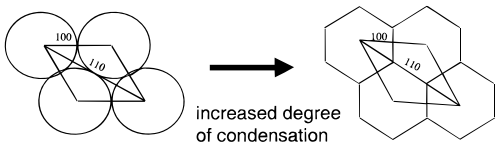

Figure 8. Schematic illustration of the structural changes of the zirconia mesostructure which occur upon condensation of the inorganic framework.

To gain further support for the proposed model of formation, XRD patterns were modeled similar to the modeling of silica structures described by Schacht et al.[20] with (Figure 9a) and without openings (Figure 10a) in the structure along the 3-fold axis. However, in this case 8-fold-coordinated Zr atoms were placed in the walls instead of 4-fold-coordinated silicon atoms. The wall was constructed in the following manner: The basis was the fluorite structure of cubic zirconia. The angles of the unit cell were slightly changed from the 90° angles, resulting in a new, distorted unit cell to lower the local symmetry. Then such individual unit cells in a full structure were replaced to form a hexagonal pore structure by moving and twisting of six units. Separate units were connected and angles and distances were adjusted using the "clean" procedure of the MSI CERIUS software package, leading to a quasi amorphous wall. Note that this does not lead to an energy-minimized structure. However, this model is sufficient to predict the XRD data. A wall thickness of 10 Å was assumed in all cases, and the total size of the cell was 45 Å × 45 Å × 10 Å. Two of the modeled XRD patterns are shown in Figures 9b and 10b. It is clearly seen that the intensities of the (100) and (200) reflections remain virtually unaffected by changes in the wall structure along the 3-fold axis, while a strong decrease in the intensity of the (110) reflection is observed, if the density of scatterers is decreased. This result supports the proposed model of formation. Further evidence in support of the proposed mechanism of wall densification is the observation that the increase in the intensity of the

(18) Chen, C. Y.; Burkett, S. L.; Li, H.-X.; Davis, M. E. *Microporous Mater.* **1993**, *2*, 27.

(19) Huo, Q.; Margolese, D.; Ciesla, U.; Demuth, D.; Feng, P.; Gier, T.; Sieger, P.; Firouzi, A.; Chmelka, B. F.; Schüth, F.; Stucky, G. D. *Chem. Mater.* **1994**, *6*, 1176.

(20) Schacht, S.; Janicke, M.; Schüth, F. *Micropor. Mesopor. Mater.* **1998**, *22*, 485.

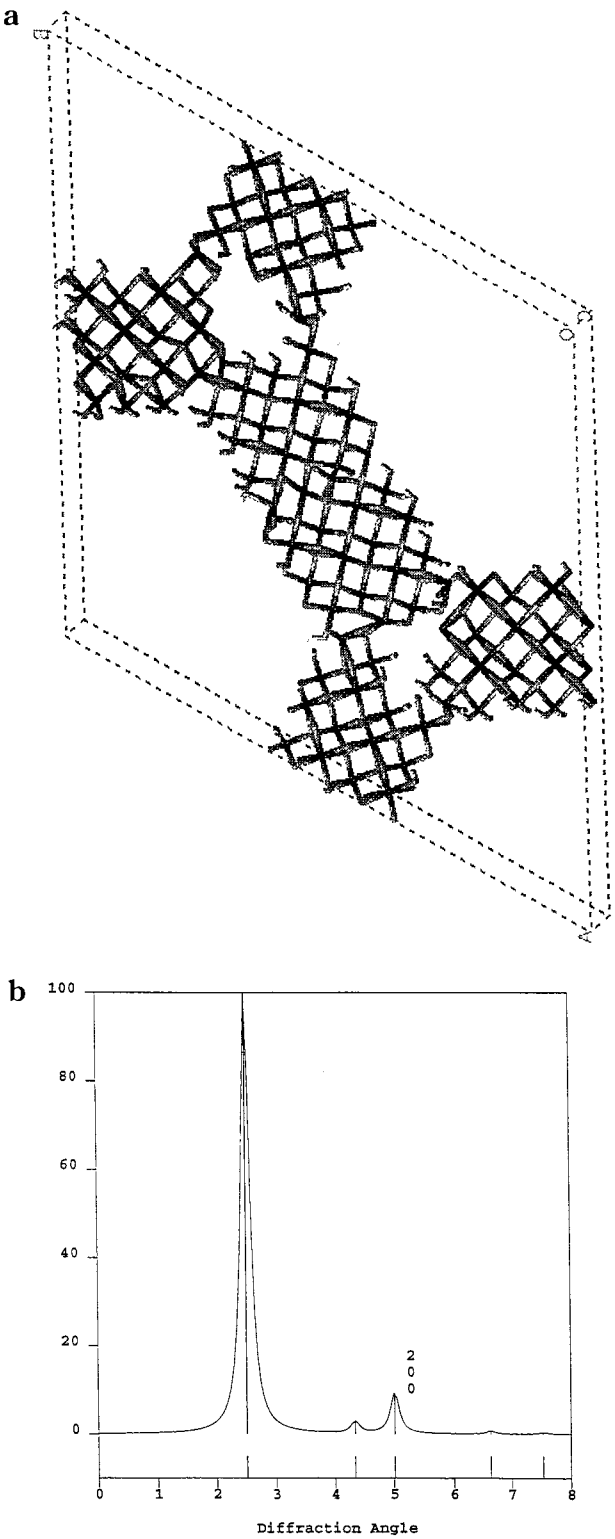

Figure 9. (a) Computer model of an unidimensional pore system of zirconium oxide with hexagonally ordered hexagonal pores with openings in the structure along the 3-fold axis. (b) Simulated diffractogram of the model shown in part a with a crystal size of 500 × 500 × 500 nm.

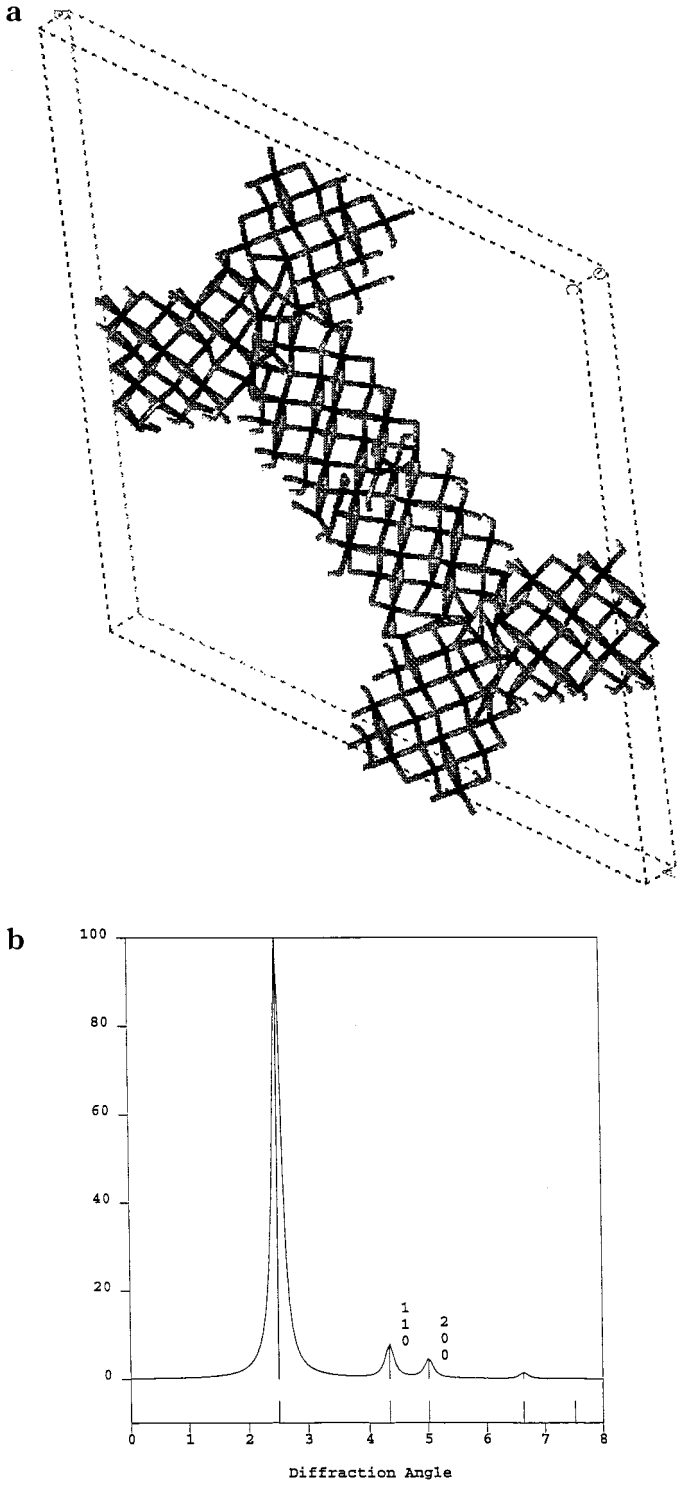

Figure 10. (a) Computer model of an unidimensional pore system of zirconium oxide with hexagonally ordered pores without openings in the structure along the 3-fold axis. (b) Simulated diffractogram of the model shown in part a with a crystal size of 500 × 500 × 500 nm.

(110) reflection is faster for Ti than for Zr, since it is well-known that the kinetics of condensation of Ti is faster than that of Zr.[15]

The mixed hexagonal/lamellar phase observed for Zr/C_{18}TABr can be explained by the higher value of the packing parameter of surfactants with a longer hydrocarbon chain. A further increase in the N_S value should favor the lamellar phase. Addition of electrolyte to the synthesis will increase the ionic strength of the solution leading to a lower a_o value and therefore to an increase in the N_s value, and therefore it is not surprising that a pure lamellar phase was observed for Zr/C_{18}TABr after addition of either HCl or NaCl.

A transition from the lamellar to the hexagonal phase has been previously observed for a particular silica mesophase and explained by Monnier et al. and Huo et

al.:[5,19] Upon aging, the increased condensation of the inorganic framework diminishes the density of anionic silanol and induces, as predicted by the charge density matching criteria, a decrease of density of the cationic surfactant. This occurs via a transition from the lamellar to the hexagonal phase. For the zirconia mesophase described herein the SO_4^{2-} ions would be expelled during the framework condensation while oxo or additional hydroxo bridges are formed between the zirconium centers; the sulfate density and thus the charge density is therefore expected to decrease during the condensation of the inorganic framework. A possible increase in the coordination number would proceed via aquo ligands under the pH conditions of the synthesis which would not change the charge distribution in the inorganic framework. The "thermally treated" sample contained actually less sulfate per zirconium atom than the "as made", which confirms the Monnier et al. model for this case. Note also that the sulfate to CTAB ratio remained unchanged (0.87 and 0.85, respectively, for the "as made" and "thermally treated" sample). This result has not been described by Monnier, but was predictable: the removing of sulfate groups during the condensation induces the expulsion of CTAB molecules from the pores in order to maintain the overall charge neutrality of the mesophase.

The different zirconia systems studied here also show that the initially formed phase is not necessarily the lamellar phase which then transforms to the hexagonal, which was sometimes assumed to be essential in the Monnier model in subsequent publications. Depending on the conditions, either phase might form first as a result of the organic−inorganic self-assembly, and the possible subsequent transformations are mainly governed by the reactions in the inorganic part of the composite, as described in detail for silica with cubic octamers as silica source.[16]

Conclusions

The mesophase formation of $Zr(SO_4)_2/C_nTABr$ and $TiOSO_4/C_{16}TABr$ has been studied as a function of surfactant chain length, salt concentration, and temperature. Rapid mesophase formation occurred immediately after mixing at room temperature, independent of the system. Depending on the surfactant chain length and ionic strength of the solution, hexagonal or lamellar phases were observed, as expected from changes in the packing parameter of the surfactant. A model of formation was developed on the basis of XRD measurements taking into account the effect of inter- and intra aggregate condensation upon heating. Non-siliceous systems are suggested to be ideal candidates for studies of inorganic−organic composite mesophase formation due to the slow condensation of inorganic species at low temperatures, allowing aggregation and condensation reactions to be studied separately.

Acknowledgment. We thank Dr. Bernd Matthiasch for the X-ray fluorescence analysis measurements and Dr. Ute Kolb for helpful discussion. We also acknowledge the financial support of the E.C. (ERB-FMRX-CT96-0084) and the DFG (Schu744/8-2).

CM991082X